SPECIAL CORE ANALYSIS LOADING CONDITIONS FOR A FRIABLE, STRESS-SENSITIVE SANDSTONE

Lindsay N. Kaye[*], James D. Hacksma[**], Sally Knudson[***], James E. Smith[**]

* Exploration and Production Consultants Limited
** Kerr-McGee Corporation
*** Kerr-McGee Oil (UK) PLC

Abstract It has been found that the conventional "overburden condition" methods of isotropically loading poorly consolidated homogeneous sandstone core material from the Gryphon Field can cause progressive sample deformation and failure during the Special Core Analysis Laboratory (SCAL) testing. Such deformations have resulted in test condition grain packings and hence porosities that are only poorly controlled and of questionable relevance to the insitu condition of the formation sampled. Anisotropic loading, with independent control of axial and confining loads on vertical plug samples has been found to result in appreciably more stable grain packing conditions. It is not possible to prove the stable grain packings obtained are representative of reservoir conditions, however, the stability of the grain packings suggests that they may be and also makes the loading procedure attractive for use in the SCA laboratory. In addition to the investigation of loading methods, sample mechanical behaviour and sonic transit time data has been gathered that calls into question the mechanical integrity of the formation at and beyond the borehole wall and hence the degree to which the responses of some borehole logging devices may be indicative of undisturbed formation characteristics in the Gryphon reservoir.

INTRODUCTION

The Gryphon Field, a normally pressured, Upper Palaeocene to Lower Eocene oil and associated gas accumulation, located on the west flank of the UK North Sea's South Viking Graben, was discovered in 1987. The reservoir sands are poorly consolidated to friable sub-litharenites with little evidence of cementation and low clay contents. The reservoir, is characterised by very high porosities (35%+) and by similarly high permeabilities (1 - 10 Darcies). The main sands are massive and have similarities with the reservoirs in the Frigg and Alba Fields.

The discovery well (Well A) was extensively cored and a comprehensive programme of SCAL tests was commissioned. The core material showed signs of mechanical disturbance (Plate 1) despite careful coring and core handling processes, including core freezing at the wellsite. Because of the extremely fragile nature of the sands, operational measures have been taken to minimise mechanical core damage

in subsequent wells. These involve the use of a specially designed brace which prevents flexing and bending during laying down of the fibre inner-corebarrel, filling the annulus between the core and the fibre inner-barrel with a liquid resin (that hardens in minutes) at the wellsite, and the use of polystyrene support profiles in the core trays during transportation. In the laboratory, core slabbing and plugging in liquid nitrogen was standard. Since both plug sample and slabbed core deformation, as an apparent result of freezing, have been noted in early wells (Plates 2 and 3), cores are no longer frozen and plugs are stored sleeved in "heat-shrink" teflon at ambient temperatures, under lease crude.

In the discovery well sampling for SCAL testing was restricted to horizontal plugs taken in intervals where there were no visible signs of mechanical disturbance. When appropriate, testing was performed at overburden conditions, stress being applied isotropically using a hydrostatic core holder. The results of so-called overburden porosity and permeability tests (up to 5000 psig) and of pore volume compressibility tests showed signs of progressive non-recoverable deformation, (Figures 1 and 2). Overburden porosity, permeability and pore volume compressibility data together with observations of sample external dimensions during and after the tests indicated significant hysteresis effects and non-recoverable unstressed property differences. The pore volume expansion/compression was not monitored for every stress cycle the samples underwent during SCAL testing. As a result, the apparent inelastic behaviour of some samples renders the accuracy of sample water saturations determined from a "base" porosity questionable.

Isotropic stressing of horizontal plugs is not a good approximation to actual anisotropic insitu stress conditions, which in the setting of the Gryphon Field can be expected to show a vertical maximum principal stress with the horizontal stresses being of a significantly lower magnitude. Density log integration together with leak-off test interpretations, borehole stability calculations and comparisons with adjacent field areas indicate overburden effective stress in the reservoir is ca. 2600 psig with maximum and minimum horizontal effective stress levels of ca. 1800 and 1400 psig respectively. It is clear that Well A "overburden" samples were exposed to confining stresses in the horizontal plane significantly in excess of those in the sub-surface.

A programme of carefully instrumented, anisotropically and isotropically loaded testing was carried out on reservoir material from subsequent appraisal wells using a modified Hoek cell (Figure 3). The cell was ported via the end plattens to allow fluid flow through the samples and to give electrical access to either p- and s-wave sources and detectors or electrical conductivity electrodes. The tests were aimed at minimising mechanical disturbance during laboratory "overburden" conditions testing, repeatably restoring the core materials to a satisfactory approximation of its insitu condition, and obtaining some understanding of the reservoir material's mechanical behaviour under stress.

RELEVANT THEORETICAL CONSIDERATIONS

In The SCA Laboratory

Permeability, relative permeability, resistivity and capillarity phenomena are all controlled to some degree by pore throat shapes and cross-sectional areas, by porosity tortuosity and, hence, in uncemented materials, by grain size, shape, sorting

and packing. It is therefore important that "overburden" SCAL testing is conducted following reversal of any grain re-ordering which occurred during coring and subsequent core and plug handling. Precise reversal of any surface mechanical disturbances experienced by the plug and the strains associated with the unstressing experienced by the core is not practical. Any mechanical disturbances suffered by the material that have caused rupture of cements cannot be reversed and any tensile strength the samples may have had in the sub-surface will be lost, although cohesive strength due to clays, if present, may be partially restored by reconsolidation.

By using vertical plug samples, independently loaded axially and in the horizontal plane, insitu stress conditions can be approximated. It is also expected that this loading approach, with careful control on deviatoric stress levels during loading and unloading will control the strains occurring and better replicate reversal of the unloading process. For SCAL tests control of strains in the plane normal to the direction of test permeability and resistivity measurements is of particular importance.

It is interpreted that during the isotropic stressing of horizontal plugs from Well A restoration of the core samples to a close approximation of their insitu grain packing arrangements, may have been incomplete because the horizontal loads exerted were excessive. Repeated isotropic cycling of the material, to successively more dense grain packing conditions, resulted in progressive changes in pore throat dimensions and grain packing. This apparent instability in porosity, pore connectivity and pore throat dimensions calls into question both the internal consistency of measurements obtained from a plug during testing as well as their applicability and relationship to the insitu reservoir material.

In The Borehole Wall

In the formation near to the wellbore, and just beyond the bit or core head, severe and complex stress distributions and anisotropies, resulting from the removal of the mass of rock of the borehole, disturb the pre-existing insitu stress field. As a result mechanical disturbance and cement rupture may occur for some distance into the formation away from the well. Estimates based upon a simple linear-elastic/Coulomb failure model for borehole wall formations (M.King Hubbert[1]) indicate that for common sedimentary rocks the lateral extent of the disturbed zone is of the order of 2 to 4 wellbore radii from the borehole wall, depending upon the elastic moduli of the formation. The disturbed zone radius may be greater if the borehole fluids penetrate the formation. The Gryphon reservoir material, more than most, fails to approximate a linear-elastic solid near the wellbore and as a consequence is subject to non-recoverable strains in the unusual stress conditions surrounding the borehole. At the low insitu stresses in the Gryphon reservoir much of the this strain can be expected to be dilationary (porosity creative). As a result of the strains the severity of the stress conditions within the borehole wall environment are progressively ameliorated. A description of the stress distribution and strain phenomena around a borehole in similar circumstances has been published by Suman[2] (Figure 4) based upon work by de Jong and Geertsma[3].

The grain packing achieved by anisotropic stressing of Gryphon sand is believed to give a reasonable approximation of the undisturbed formation. Thus, in the laboratory we have attempted to recreate the insitu stress and grain packing condition before drilling, or some distance away from the borehole. It may not, however, be possible to directly compare core data obtained in this way to log responses,

particularly of tools with a shallow depth of investigation, since these will primarily respond to the disturbed near-wellbore formations under reduced stress conditions (Figure 4).

If mechanical disturbance of the borehole wall rock is accompanied by dilation of the pore volume (Suman[2]) then the additional fluids occupying this additional pore space should be considered. Since the borehole mud pressure is kept at an over-balance with respect to formation fluid pressure, it is most likely that this additional fluid will come from the borehole, resulting in extra filtration loss or possibly even whole mud invasion.

The mechanical disturbance of weak or brittle rocks near to the wellbore will affect the deep reading resistivity (Rt) device least, but could, if the damage zone were deep, influence sonic, nuclear and micro-resistivity log data. Such logs would not be reading incorrectly but simply responding to formation that is not representative of the native state reservoir, to which the deep-reading resistivity log is hopefully responding, and which the application of core loading in "overburden" testing is seeking to replicate.

SEQUENCE AND PROGRAMME OF LABORATORY TESTING

Well B

Sample preparation

Plug freezing damage was extensive in the 38mm x 76mm plugs initially selected for testing. Samples were selected to avoid areas where there were visible signs of mechanical damage. After frozen storage the selected samples were found to be in very poor condition, being broken or showing signs of cracking and surface spalling (Plate 3). Where undamaged sample volumes were considered sufficient for viable testing, it was impossible to load even these into the Hoek cell since they were up to 5mm 'over-sized' in the diameter. Since sample lengths were not measured after plugging and trimming, axial expansion/contraction cannot be speculated upon. Such phenomena have been reported in unconsolidated sands, particularly where significant quantities of water are trapped in the plugs or when large quantities of clay minerals are present[4], neither of which is the case in the Gryphon plugs.

In order to avoid the same thing happening again, sleeved samples were specified for future anisotropically loaded testing. This requires taking 36mm o.d. (nominal) plugs such that with sleeving they can still be loaded in the modified Hoek cell apparatus. Plug samples are also no longer stored in a frozen state in order to avoid any progressive disturbance due to temperature effects on the sample material or on the heat shrink sleeving.

Test procedure

One sample from Well B did not show a severe increase in diameter. After transverse breakage its constituent parts were individually considered too short for standard testing purposes. However, two trimmed samples ca. 47.5mm long were obtained and tested as a guide to the selection of loading and testing parameters for future testing. Sample 'a' was subjected to cyclic isotropic stressing and to a form of

drained triaxial strength test. Sample 'b' was subjected to cyclic anisotropic stressing. Sample 'b' failed due to poor axial loading control and only a limited amount of data was gathered.

Wells C and D

New core handling methods had been introduced for the Well C and D cores, aimed at reducing the incidence of mechanical disturbance at the wellsite and during transportation and reception at the laboratory. Much of the core shows the benefit of this special handling, although severe disturbance is often evident at the bases and tops of cored intervals (Plate 4).

Twelve plug samples were selected from Well C, avoiding the zones of disturbance referred to above and any other evident physical anisotropies. These samples, by comparison with near-by conventional core plug data, were expected to represent a reasonable cross-section of reservoir properties. Five samples were selected from Well D with which to confirm the test results obtained from the Well C samples. These samples were taken from the whole core 'blind', i.e. before slabbing, and as a result did contain some textural anisotropies. Sample details together with their post-testing porosity and permeability values are set out in Table 1.

TABLE 1 Sample details.

Well	Sample No.	Test Conditions	Porosity %	Grain Density g/cc	Permeability mD
C	1G	Iso	33.4	2.66	7060
	2G		33.2	2.66	5180
	6G		34.8	2.66	8890
	10G		36.7	2.66	9030
	3G	Aniso	30.0	2.67	1670
	6GA*	A	31.3	2.66	9100
	9G		34.0	2.67	6780
	11G		36.3	2.66	6680
	4G	Aniso	33.7	2.65	4910
	5G	B	36.9	2.66	8920
	7G		37.2	2.65	7640
	8G		37.6	2.66	8960
D	1	Aniso	33.3	2.66	4980
	G1		32.5	2.66	5433
	G2		31.9	2.66	5515
	3		31.4	2.67	2020
	4		25.3	2.66	464

* Sample 6GA failed before deformation testing.

Sample preparation and base parameter measurement

To avoid sample freezing damage, as observed on samples from Well B (Plate 3), 36mm o.d. plugs were taken, sleeved in heat shrink teflon and stored at ambient temperatures under lease crude. The sleeved 36mm x ca. 75-80mm samples were all end-trimmed to have parallel ends within the tolerances allowed by such a friable material. Each sample was measured by calipers and then mounted in the Hoek cell and isotropically loaded to a 'zero point' of 100 psig, to take up any surface irregularities in the samples and to avoid fluid by-pass during permeability testing. At the 'zero point' each sample was flushed with mineral oil (kerosene) until the effluent was clean. No other cleaning was carried out at this stage.

After testing the samples were demounted, examined for any evidence of physical disaggregation or failure, and then were cleaned by refluxing in a low-boiling point azeotrope methanol-dichloromethane to remove any residual oil and salts present. The plugs were then dried to constant weight in a humidity oven at 40°C and 40% relative humidity before being measured by calipers for external dimensions, for grain volume in a helium expansion Boyle's Law porosimeter, and for air permeability in a Hassler cell at 100 psig cell pressure.

Test procedure

Testing was initially conducted using the twelve samples from Well C. The samples were divided into three sets of four. The loading conditions under which testing took place was different for each set (Table 1).

In accordance with common laboratory practice[5], which requires that samples for "overburden" testing be stressed up to the value of the vertical effective stress, the isotropic control sample set was tested at 2600 psig confining pressure. The anisotropic sample Sets A and B were tested at an axial load of 2600 psig and jacket pressures of 1800 and 1400 psig, respectively.

Based upon experience gained from the failed Well B samples, the isotropic loading and unloading was controlled to maintain a fixed ratio of axial and jacket pressures throughout to avoid any excessive deviatoric stresses developing accidentally (Table 2 and Figure 5). Similarly, it had also been established that a strain to loading rate sensitivity could exist in the Gryphon material. In accordance with these observations and experience gained with other granular materials an axial loading/unloading rate of 10 psi/second was specified for all loading conditions. A three minute halt in the loading process was allowed at each step (Table 2) for initial 'creep' phenomena to develop. Two such loading/unloading cycles were specified with a one hour period allowed for more extensive 'creep' monitoring at both peak and 'zero point' stress conditions.

During loading and unloading plug deformation was monitored by recording changes in pore volume and axial strain. Pore volume changes were measured by liquid squeeze out/return to/from a micro-burette and axial strains were recorded using a vernier scaled caliper device sensitive to displacements of 1 micron operating on the end plattens. Load testing against metal blanks, prior to tests on Well B samples, had provided information concerning dimensional changes in the equipment configuration during testing. Figure 6 illustrates the form the recorded testing results take.

TABLE 2 Stress levels for stepwise anisotropic loading and unloading cycles.

Axial Load (psig)	---Jacket Pressure (psig)--- Set A	Set B
0	0	0
100	100	100
200	200	200
350	300	
400		300
500	400	
600		400
650	500	
800	600	500
950	700	
1000		600
1100	800	
1200		700
1250	900	
1400	1000	800
1550	1100	
1600		900
1700	1200	
1800		1000
1850	1300	
2000	1400	1100
2150	1500	
2200		1200
2300	1600	
2400		1300
2450	1700	
2600	1800	1400

Kerosene liquid permeability measurements were carried out at first loading cycle zero and peak stress points, second loading cycle zero (end of first cycle residual point), and peak stress points and final zero stress point (end of second cycle residual point). In tests carried out on Well C anisotropic Set B (and subsequently on the Well D material), flow reversal checks were made to establish if any fines migration was affecting measured liquid permeabilities and none was indicated. In addition measurements of shear and compressive wave propagation times were taken at each cycle's peak loading condition.

The results of the testing of Well C material indicated that the anisotropic Set B samples had undergone the most stable deformations, with least hysteresis indicated in the second loading and unloading cycle. This was judged on the basis of simple acceptance criteria, i.e., the least difference between the first and second loading

cycle (3 minute) peak volumetric and axial strains and the minimisation of the end-second-cycle residual strain values. For each sample in anisotropic Set B an apparently stable grain packing condition was achieved at the peak of the first loading cycle which was closely repeated at the peak of the second loading cycle. It was, therefore, decided to test Well D, material under the same loading conditions as Set B using the same simple acceptance criteria to determine comparability with the data from Well C.

Rock deformation testing

The core material remaining on completion of the primary testing was used to obtain some indications of residual strength characteristics and of rock mechanical parameters for the computation of borehole and perforation stability. In this testing all samples were anisotropically loaded dry, with no saturating oil phase present, but otherwise as per the anisotropic Set B loading programme (Table 2). In each set, each sample was stressed to a different load target (Table 3). Once loaded the jacket (confining) pressure was lowered in 200 psi steps, at 10 psi/second, as per the other loading/unloading cycles, and axial loads and axial strains were monitored.

TABLE 3 Initial loading conditions for deformation tests.

Load Target	Jacket Pressure (psig)	Axial Pressure (psig)
A	400	600
B	800	1400
C	1200	2200
D	1600	3000

TEST PROGRAMME RESULTS AND INTERPRETATION

Well B

The results obtained from the two undersized samples are summarised in Figures 7, 8 and 9. It should be borne in mind that the samples were not of the standard 2:1 length to diameter ratio usually required for core testing and that the results can, therefore, only be used as qualitative indicators of the material's mechanical behaviour under stress. Direct quantitative comparison with later test results may be misleading.

Sample 'a'

Cycling Sample 'a' at low levels of isotropic stress (250 psig) gave rise to severely hysteretic plug deformation behaviour which decayed to only minor hysteresis levels

in 4 cycles. Thereafter limited hysteresis continued, with progressive deformation occurring for a further 7 cycles, without achieving closed-loop (stable) hysteretic behaviour. Further cycling at increasing levels of isotropically applied stress (500, 750 and 1000 psig) showed additional evidence of open-loop (unstable) hysteresis and a large residual (non-recoverable) strain was developed. The 1000 psig peak pore volume change was 2.82 cc which is estimated to represent 5.25 porosity units (p.u.) or a 13% reduction in initial porosity. Only 0.82 cc of this pore volume reduction was recovered by sample unloading, and of the residual pore volume reduction (2.00 cc/3.7 p.u.), only 0.4 p.u. were due to axial dimensional changes. The remainder was apparently due to substantial strains in the horizontal plane, which are calculated to have reduced the mean sample diameter by ca. 600 microns. This cross-sectional change must have resulted from a major reordering of grains and influenced pore throat areas considerably.

Volumetric and axial strain results, from the drained triaxial test, demonstrate that the isotropically stressed material performs as a linear elastic solid until confining pressure drops below 800 psig (Figure 8). Above 800 psig it is presumed that grain strains are released without mechanical disturbance of the sample. As the confining pressure is further released the material relies more and more upon the angle of internal friction to assist in supporting the axial load and hence in limiting axial strains. This results in incremental volume strains due to dilation of the core material of the order of 1 cc (ca. 2 p.u.). Below 100 psi jacket pressure complete sample failure occurs and uniaxial compressive strength falls to close to zero as confining pressure is released.

Sample 'b'

For Sample 'b', only 2.5 cycles of low intensity anisotropic stressing to 300/200 psig are required before closed-loop (stable) deformation behaviour was accomplished. At this peak the sample had suffered only 0.86 cc (1.5 p.u.) of porosity reduction for an axial length change of 149 microns compared to which the most stable Sample 'a' peak was recorded after 1.38 cc of squeeze out (2.4 p.u.) for an axial length change of 210 microns. Apart from the earlier sample stability achieved, these results also suggest a reduction of strains in the horizontal plane during the low stress level anisotropic cyclic stressing compared to the isotropic stressing. Both stress conditions are comparable with the stress levels commonly used in conventional core analysis routines in Hassler cells.

The accidental overstressing of Sample 'b' allows one approximate Mohr's circle to be drawn (see Figure 9) which is consistent with the mechanical performance evident from a modified drained triaxial test carried out on Sample 'a'. Therefore the results, which show no apparent tensile strength and a minimal unconfined uniaxial compressive strength, are not surprising. However the tolerance to axial loads increases rapidly with increasing confining stress, indicating effective angles of internal friction as high as 45° or more. The failure envelope indicated by the 45° and 23.5° lines in the Mohr's Diagram (Figure 9) was used to calculate (with a conservative factor of safety) the approximate upper limit of allowable deviatoric loading shown on Figure 5.

These test results were all obtained with the sample saturated with mineral oil. Apart from sample size considerations, these data are only qualitatively comparable with the later triaxial testing of failure conditions, which for convenience and speed

were conducted dry on cleaned samples.

Wells C and D

The format for the presentation of strain versus stress measurements is as set out in Figure 6. Table 4 compares the 3 minute peak value between the first and second loading cycles and the second loading cycle residual values of pore volume reduction and axial strain.

TABLE 4 Peak differences and residual values for Wells C and D.

			3 Minute Peak Difference ----2nd vs 1st Cycle----			Residual Value ----End 2nd Cycle----		
Well	Test	Sample	Volume cc	Length u	p/f	Volume cc	Length u	p/f
C	Iso	1G	-0.322	+141	f	0.122	97	f
		2G	+0.074	+26	p	0.100	45	p
		6G	-0.347	+158	f	0.330	165	f
		10G	+0.225	+167	f	0.235	107	f
	Aniso A	3G	-0.003	+8	p	0.000	2	p
		6GA	+0.182	+166	f	0.382	112	f
		9G	+0.060	+125	p	0.148	30	p
		11G	-0.007	+124	p	0.088	81	f
	Aniso B	4G	+0.026	-14	p	0.075	1	p
		5G	+0.034	+10	p	0.181	-8	p
		7G	+0.229	+128	p?	0.180	53	p?
		8G	+0.078	+20	p	0.150	21	p
D	Aniso	1	-0.091	+44	p	0.030	38	p
		G1	-0.306	+8	f	-0.250	6	p?
		G2	-0.349	+6	f	-0.526	-256	f
		3	-0.457	-44	f	0.154	-39	f
		4	-0.028	+24	p	0.069	6	p

p = pass, f = fail w.r.t. hysteresis criteria

The reduction in peak difference and 2nd cycle residual values for both volume and length measurements indicate a general improvement in deformational stability as the anisotropy of the loading/unloading sequence is increased, even though some sample integrity problems appear to have affected the Well D results. The Well D results were disappointing since two of the samples clearly failed to achieve a stable grain packing condition (G2 and 3) and one (G1) was a marginal case. In the case

of sample G2 the plug was damaged at the ends and required significant dressing to less than the nominal 75mm length for testing and in sample 3 there was an organised system of parallel, partially-cemented shears at approximately 30 degrees to the plug axis, which would certainly have influenced the mechanical behaviour. Similar features were seen in sample 4 but are randomly oriented, well-cemented and do not appear to have influenced the stability of the plug appreciably.

In order that similar standards of acceptable loading behaviour could be applied to future Gryphon material testing, pre-testing 3 minute peak stress and post-testing zero stress values of volume and length change criteria have been adopted (Table 5). These criteria restrict the maximum acceptable shift between cycle peaks or zero points to less than -0.5% of pore volume and -0.125% of sample length. Allowance has been made for zero point drift and peak stress equipment strains obtained during tests using metal blanks. To date no significant numbers of samples stressed anisotropically have been shown to have suffered deformations beyond these criteria in any of the SCAL testing carried out on material from wells subsequent to Well C.

TABLE 5 Hysteresis acceptance criteria.

Pre-test 3 minute peak:		
125 to -25 microns	=	-0.15 to + 0.03 p.u.*
0.25 to -0.10 cc	=	-0.30 to +0.12 p.u.
Post-test zero point residual:		
50 to -10 microns	=	-0.063 to +0.01 p.u.
0.20 to -0.10 cc	=	-0.25 to +0.12 p.u.

* Assuming a porosity of 35% and a sample volume of 80 cc.

Permeability and pore compressibility data

Oil permeability values were seen to be affected by the application of stress to the samples but no systematic reduction trends or comparisons between first and second cycle values were evident (Table 6). To some extent this may be due to sample clean-up caused by the continuing kerosene flooding during permeability testing and possibly also to the flushing out of fines. It is apparent, however, that these crudely measured liquid permeabilities were only marginally sensitive to the type of loading conditions employed. This in itself does not ensure that relative permeability measurements will not be.

Using data obtained from the main testing sequence, second cycle rates of pore volume reduction with increasing load have been established, from which pore volume compressibilities have been calculated (Table 7). These are of the same order of magnitude as the uniaxial compressibility values obtained using conventional hydrostatic methods and the Teeuw correction[6] (Poisson's Ratio = 0.3) on Well A core material. However, the measured compressibility is a response to increasing both axial and confining loads and is, therefore, likely to be less than true uniaxial values at the same stress level. Specifically designed pore pressure reduction tests at higher total stress levels would be required to obtain more refined data.

TABLE 6 Summary of oil permeabilities.

Well	Sample No.	K air mD	Oil Permeability (mD)			
			First Cycle		Second Cycle	
			Zero Pt.	Peak	Zero Pt.	Peak
C	1G	7060	1965	1485	1557	1475
	2G	5180	2569	2091	2200	2093
	6G	8890	5617	3510	3661	3475
	10G	9030	3288	2680	2779	2665
	3G	1670	667	573	677	650
	6GA	9100	4609	2788	3166	2715
	9G	6780	3214	2734	2822	2688
	11G	6680	3063	2364	2688	2428
	4G	4910	1478	1414	1637	1488
	5G	8920	4323	3757	4101	3789
	7G	7640	3200	1163	1378	1041
	8G	8960	2678	1828	2447	2018
D	1	4980	1485	1187	1265	1128
	G1	5455	1608	1176	1386	1351
	G2	5515	2484	1649	1926	1634
	3	2020	716	515	607	517
	4	464	150	96	124	97

From measured pore volume reductions during the stress cycling 'initial unstressed' to 'overburden' porosity corrections have been calculated (Table 8). A correction factor of ca. 0.94 - 0.95 for the most stable test results is indicated. This compares with an average value of 0.96 measured on isotropically stressed (to 3100 psig) dry samples from Well A. The fluid saturated values obtained during the course of the anisotropic stress cycling are thought to be more reliable. Unsaturated samples tend to exhibit higher internal frictional effects, which limit pore volume reductions, and the grain packing achieved by isotropic stressing is considered less representative of the undisturbed formation than that achieved with the anisotropically stressing. The range of the data of 0.898 - 0.985, however, indicates that the validity of a blanket correction is very much dependent upon the initial state of disaggregation of the sample. Caution should, therefore, be exercised when applying such 'blanket' corrections to conventional core data.

The same data set can be compared to the axial strains associated with the pore volume reduction (Table 8). Axial strains of up to 1% appear to be typical of the 5 - 6% pore volume reduction in the stable tests. The degree of axial to pore volume strain is presumably dependent upon the initial state of sample disaggregation and

cannot in this small sample set be used to interpret the dominant direction (axis or diameter parallel) or mechanism of reconsolidation.

TABLE 7 Pore volume compressibility at 2nd cycle peak.

P.V. = Pore Volume Comp = Compressibility
B.V. = Bulk Volume Phi = Porosity
Pk = Peak Resid = Residual

Well	Sample No.	Phi %	Final P.V. cc	2nd Pk-Res PV Diff. cc	P.V.at 2nd Pk cc	2nd Cycle Slope cc/psi $x10^{-4}$	P.V. Comp psi $x10^{-5}$	p/f
C	1G	33.4	26.558	1.086	25.472	3.125	1.227	f
	2G	33.2	26.753	1.080	25.673	3.175	1.237	p
	6G	34.8	28.111	1.375	26.736	2.675	1.001	f
	10G	36.7	31.391	0.925	30.466	2.550	0.837	f
	3G	30.0	24.285	0.880	24.405	2.000	0.855	p
	6GA	31.3	24.016	1.068	22.948	3.750	1.634	f
	9G	34.0	32.202	0.961	31.241	2.600	0.832	p
	11G	36.3	26.458	0.706	25.752	2.500	0.971	f
	4G	33.7	25.443	0.696	24.747	1.875	0.758	p
	5G	36.9	26.544	0.598	25.946	2.500	0.964	p
	7G	37.2	27.085	0.879	26.206	2.525	0.964	p?
	8G	37.6	28.599	0.780	27.819	2.475	0.890	p
D	1	33.3	29.391	0.780	28.611	2.500	0.874	p
	G1	32.5	27.573	1.369	26.204	3.200	1.221	f?
	G2	31.9	23.383	1.536	21.847	2.500	1.144	f
	3	31.4	29.013	0.821	28.192	2.000	0.709	f
	4	25.3	23.671	0.770	22.901	2.750	1.201	p

p = pass, f = fail w.r.t. hysteresis criteria

Sonic transit time data

Sonic transit times measured on each sample at peak stress conditions are shown in Table 9. These were not expected to show much, if any, variation between first and second loading cycle peaks, and indeed do not. However, regardless of loading condition, they all indicate faster compressive wave velocities and substantially faster shear wave velocities than indicated from sonic logs and from the analysis of sonic waveforms. This unfortunately limits the degree to which these data can be used for correlation to log data and for extrapolation via log data to other localities in the wells.

TABLE 8 Linear and pore volume strains.

Well	Sample No.	--2nd Cycle Peak-- Length mm	Pore Vol cc	Length Change mm	Pore Vol Change cc	Length Strain %	Volume Strain %	p/f
C	1G	79.3	25.472	0.878	1.655	1.11	6.10	f
	2G	80.0	25.673	0.387	1.758	0.48	6.41	p
	6G	85.8	26.736	0.941	2.722	1.11	9.24	f
	10G	79.5	30.466	0.910	2.275	1.14	6.95	f
	3G	85.1	24.405	0.262	1.390	0.31	5.39	p
	6GA	81.2	22.948	1.174	3.193	1.45	12.21	f
	9G	87.9	31.241	0.447	1.859	0.51	5.62	p
	11G	78.1	25.752	1.354	2.253	1.73	8.04	f
	4G	79.6	24.747	0.847	1.522	1.06	5.79	p
	5G	75.5	25.946	0.174	1.536	0.23	5.59	p
	7G	77.0	26.206	0.760	2.980	0.99	10.21	p?
	8G	78.4	27.819	0.748	1.540	0.95	5.25	p
D	1	90.2	28.611	0.319	1.519	0.35	5.04	p
	G1	84.6	26.204	0.139	1.270	0.16	1.48	f?
	G2	75.5	21.847	0.267	3.550	0.35	13.98	f
	3	89.9	28.192	0.372	1.152	0.41	3.93	f
	4	91.0	22.901	0.380	2.697	0.42	10.47	p

p = pass, f = fail. w.r.t. hysteresis criteria

Compressive and shear wave interval transit times of 85 - 125 and 210 - 250 microseconds/ft respectively for Well C and 85 - 135 and 185 - 225 microseconds/ft respectively for Well D have been calculated from the Array Sonic results. These data compare with laboratory values of 90 - 116 and 140 - 185 microseconds/ft respectively for Well C and 92 - 103 and 140 - 170 microseconds/ft respectively for Well D. Compressive to shear wave velocity ratios, of 1.65 - 2.20 have also been calculated from log results whereas, values of 1.45 - 1.66 were measured in the laboratory. In each case, however, the logged shear velocity value approaches that of the mud and is very unreliable. Calculated 'Dynamic Poisson's Ratios' from logs are 0.22 - 0.39, which range across the typical sand to shale range of values. The laboratory results indicate values in the range 0.08 - 0.215 which are distinctly sand-typical (granular material). The laboratory values are also consistent with the results of both the deformation testing and of borehole stability analyses, indicating a material with potentially high angles of internal friction and of high compressive strengths achieved at low confining pressures.

These observations all tend to indicate that the sonic logs must be severely influenced by a zone of formation deformation and of consequent stress reduction

around the wellbore. If laboratory compressive wave values are considered representative of the insitu undisturbed formation, then calculations show the sonic log is affected by mechanically damaged formation, possibly to a depth of investigation of to 5" to 18" (max) (Table 9).

TABLE 9 Summary of acoustic velocity measurements.

Well	Sample	First Cycle		Second Cycle		Log Reading		Depth of Investi-gation (inches)
		Vp	Vs	Vp	Vs	DT	DTL	
		usec/ft						
	*							
C	2G	108.2	163.1	107.4	164.5	116	113	9.6 - 11.6
	3G	99.9	145.5	98.9	145.1	106	105	10.3 - 11.3
	9G	105.7	162.6	105.3	160.5	115	114	11.8 - 12.5
	4G	101.2	154.0	100.8	153.3	111	105	8.5 - 13.2
	5G	107.5	171.0	107.1	162.4	117	116	11.8 - 12.5
	7G	114.9	171.8	114.2	170.7	120	117	6.5 - 9.4
	8G	111.8	165.0	114.0	168.8	118	116	5.3 - 6.7
D	1	100.1	165.6	99.7	165.6	120	119	17.8 - 18.2
	4	92.1	139.2	92.1	140.2	97	96	8.5 - 9.6

*Only for samples passing the hysteresis acceptance criteria

Mechanical behaviour data

Drained (atmospheric pore fluid pressure), dry-state triaxial tests were carried out on all the Wells C and D material. The samples were not resaturated with mineral oil after the porosity and air permeability measurements, so the results may be expected to show slightly higher angles of internal friction compared to the Well B oil saturated sample results. Typical results, illustrated in the form of Stress versus Strain graphs and Mohr's Diagrams, are set out in Figures 10 and 11.

The common indication of all the results is that samples stressed to anisotropic stress levels, approaching those predicted for the undisturbed reservoir, initially perform in a linear-elastic mode as grain strain occurs. The samples then fail progressively by dilatant shear at high apparent angles of internal friction as confining stress is reduced. Samples stressed to the higher initial stress levels are able to withstand much higher levels of axial load at lower confining pressures resulting in apparent values of the angle of internal friction of 54 - 63°. From lower initial stress levels dilatant shear failure occurs much earlier in the unloading, or immediately, and at lower apparent angles of internal friction. This difference is interpreted to be due to achieving a more stable grain packing density at the higher initial stress levels. The results also tend to suggest that only very low confining pressures (mud pressures?) are required to satisfy the borehole stability requirements of uniaxial compressive strengths in the near wellbore formation.

CONCLUSIONS

Testing of the Gryphon core material under a range of loading conditions has demonstrated that:

1. Isotropic stressing and stress cycling, at stresses as low as 250 psig, can cause progressive plug deformation in unconsolidated materials and can result in irregularities in assumed values of porosity.

2. Anisotropic stressing and stress cycling of vertical homogeneous plug samples, up to values approximating the insitu effective stress regime, can limit the progress of deformation and appears to result in stable grain packing conditions almost immediately.

3. The repeatable stability of the grain packing achieved by anisotropic loading allows SCAL testing to be conducted on samples with stable porosity characteristics.

4. Porosity corrections obtained from a comparison of conventional and special core analysis results, even if obtained under anisotropic loading conditions, may be sensitive to the initial degree of sample disaggregation and should be used with caution.

5. Unconsolidated materials may deform by dilatant processes in the near borehole formation, as a result of which, shallow reading log responses may be affected.

6. Anisotropically loaded test results may be difficult to correlate to log data if shallow reading logs are affected by mechanical disturbance of the near-wellbore formation.

7. Granular materials may develop very high uniaxial compressive strengths under very low confining pressures and render borehole conditions stable for drilling and logging purposes.

REFERENCES

1. Hubbert,M.K. and Willis,D.G.: "Mechanics of Hydraulic Fracturing," *J.Pet.Tech.* (June 1957) 153-66.
2. Suman,G.O.Jnr.,: "Unconsolidated Sand Stabilisation Through wellbore Stress Control," *Proc. 50th Annual Fall Meeting, SPE, Dallas* (Sept 1975) SPE 5717.
3. de Josselin de Jong,G. and Geertsma,J.: "De Sapnnings-verdeling Rondom Verticale In Zandige Dekterreinen Geboorde Holten In Stand Gehouden Door Zware Vloeistof," (Feb. 27 1953) *De Ingenieur.*
4. Torsaeter,O. and Beldring,B.: "The Effect of Freezing of Slightly Consolidated Cores," *SPE Form. Eval.* (Sept. 1987 357-60.
5. Keelan,D.: "Special Core Analysis," Core Laboratories Inc. 1982.
6. Teeuw,D.: "Prediction of Formation Compaction from Laboratory Compressibility Data," *Proc. 45th Annual Fall Meeting, SPE, Houston* (October 1970) SPE 2973.

ACKNOWLEDGEMENTS: Thanks are due to Bart deBoer of Exploration and Production Consultants Limited for his work on the Well A core analysis results, to Iain McNeil of the Geochem Group for his work on the initial anisotropic loading equipment and trials, to Rob Evans of the Robertsons Group for implementing "production" facilities for anisotropic loading of Gryphon material subsequent to Well C, to Oliver Skelton of Schlumberger for his useful discussions concerning the Array Sonic log responses, and to the Kerr-McGee management in both London and Oklahoma City and the Gryphon partners (Aran, Clyde, Santa Fe and Fina) for permission to publish this paper.

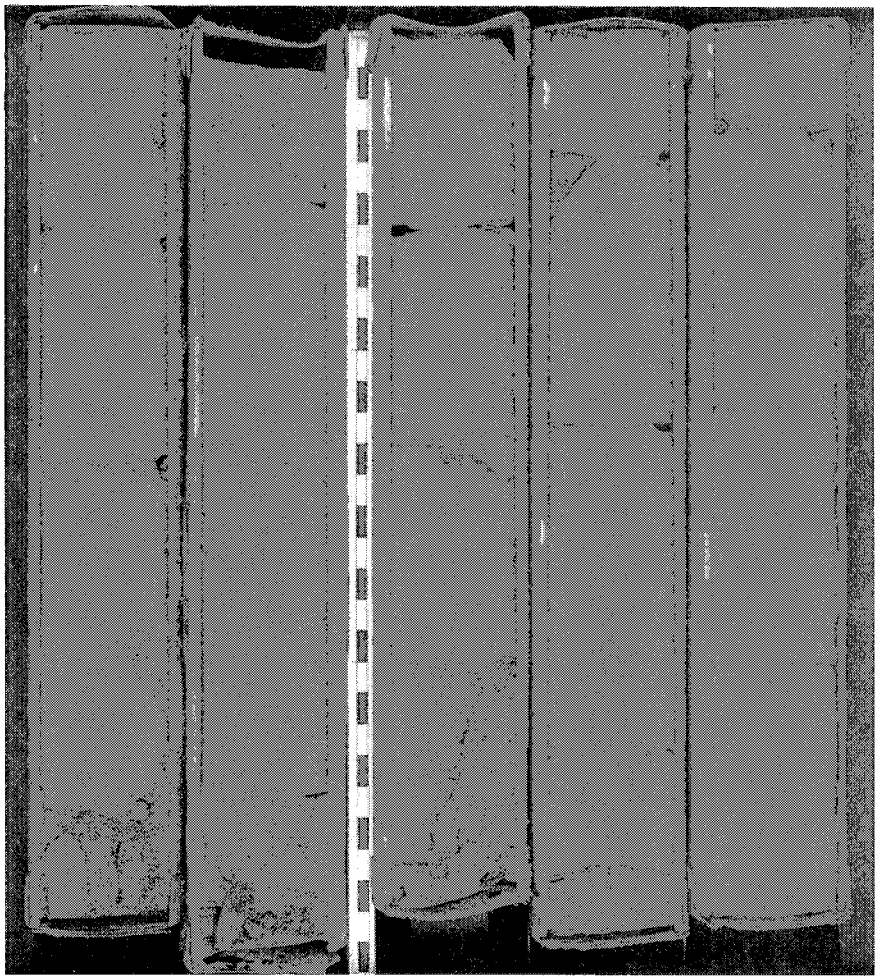

Plate 1 Core Damage (Well A)

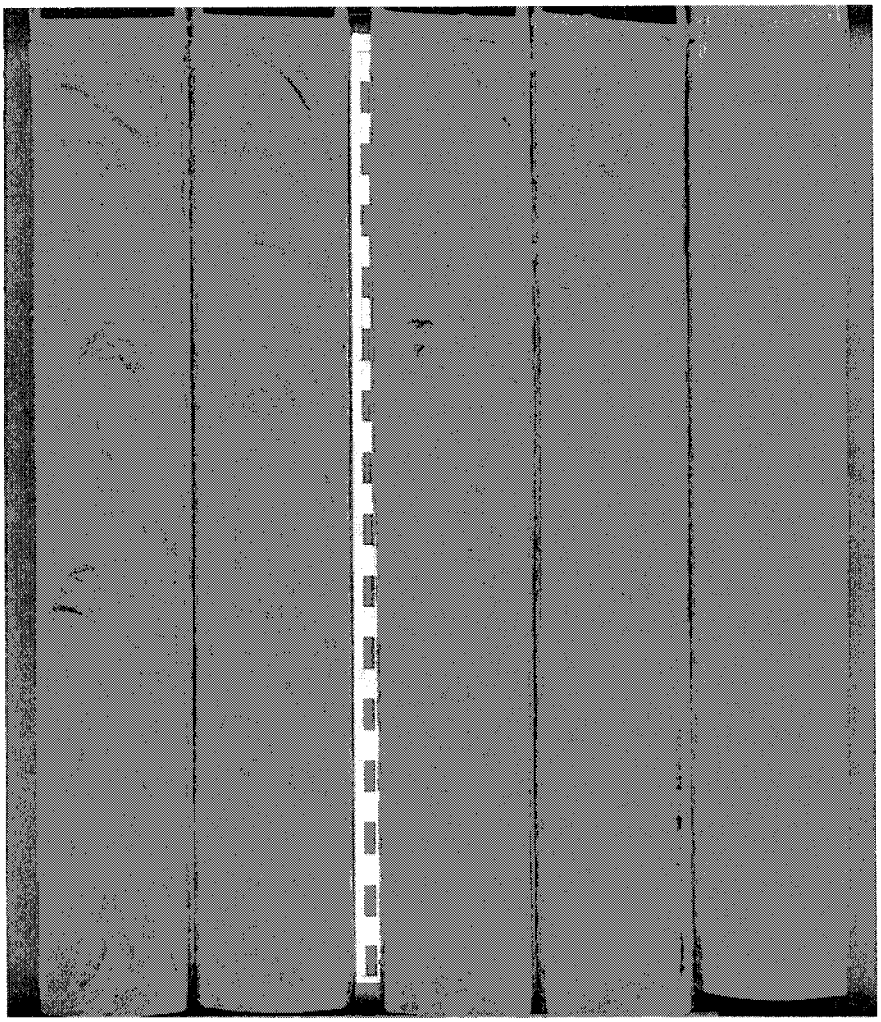

Plate 2 Core damage accentuated by freezing (Well C)

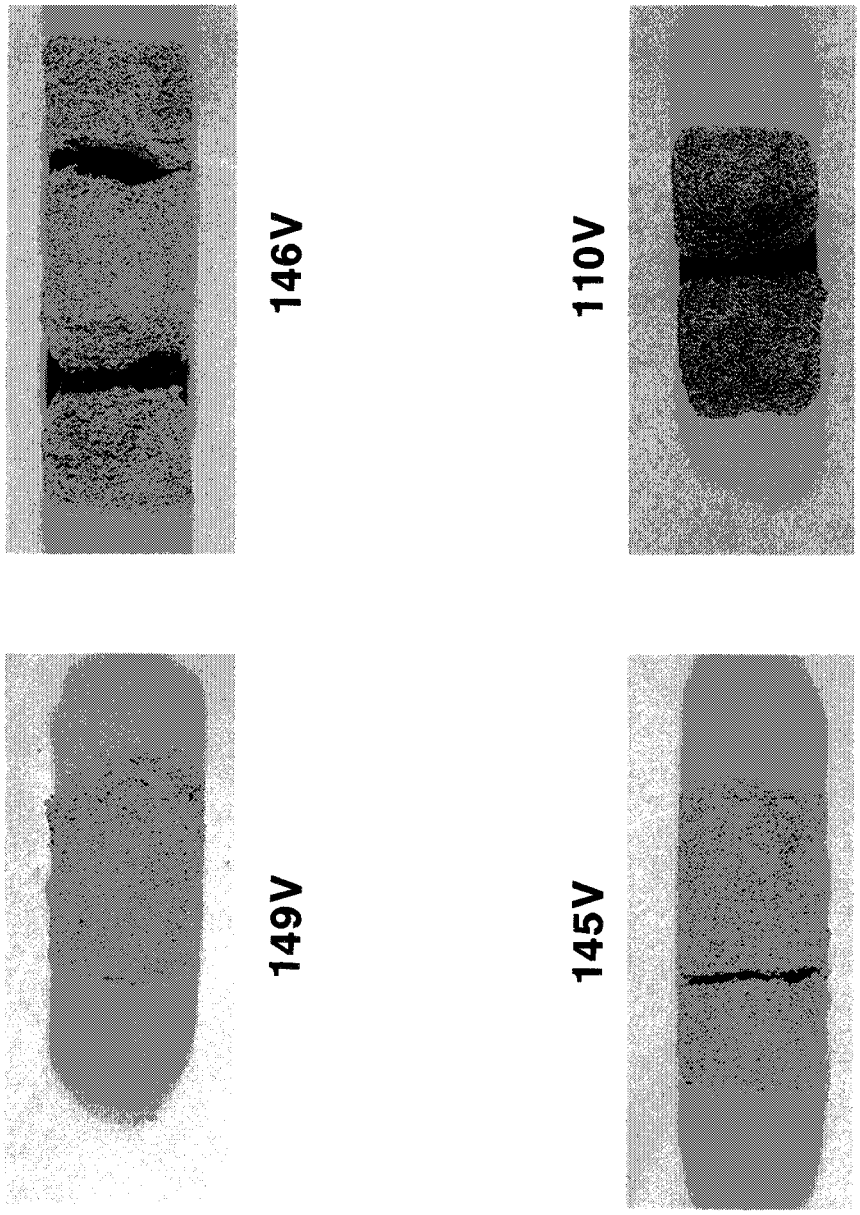

Plate 3. Plug freezing damage - Well B

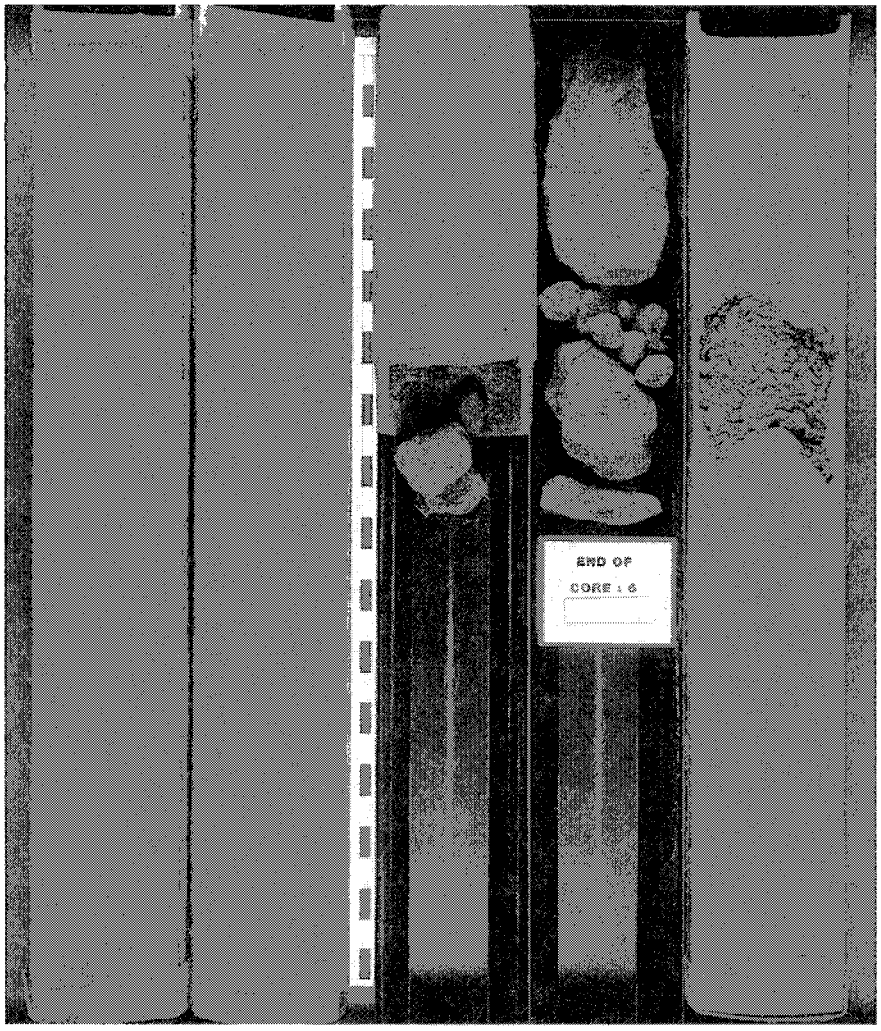

Plate 4 Top and base core deformation (Well C)

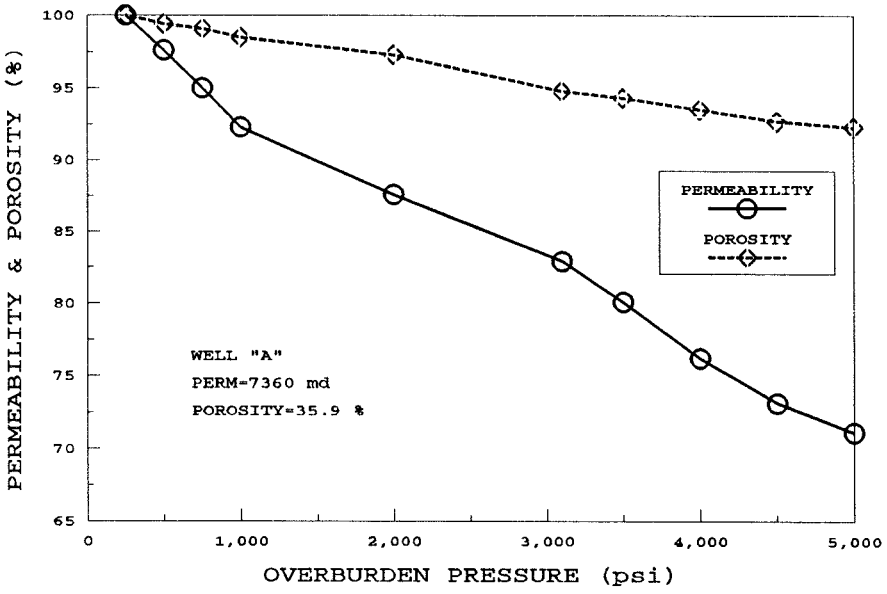

FIGURE 1 **Air permeability and helium porosity as a function of overburden pressure.**

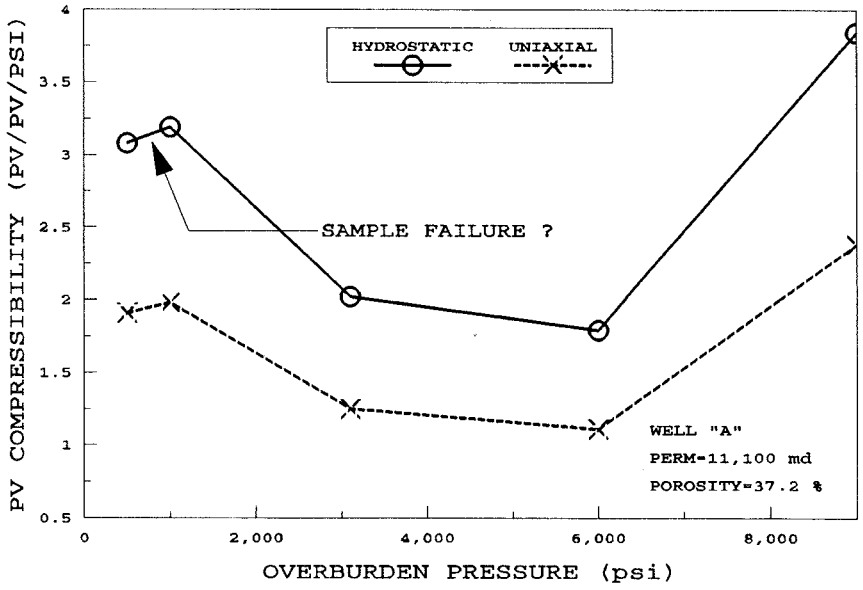

FIGURE 2 **Pore volume compressibility as a function of overburden pressure.**

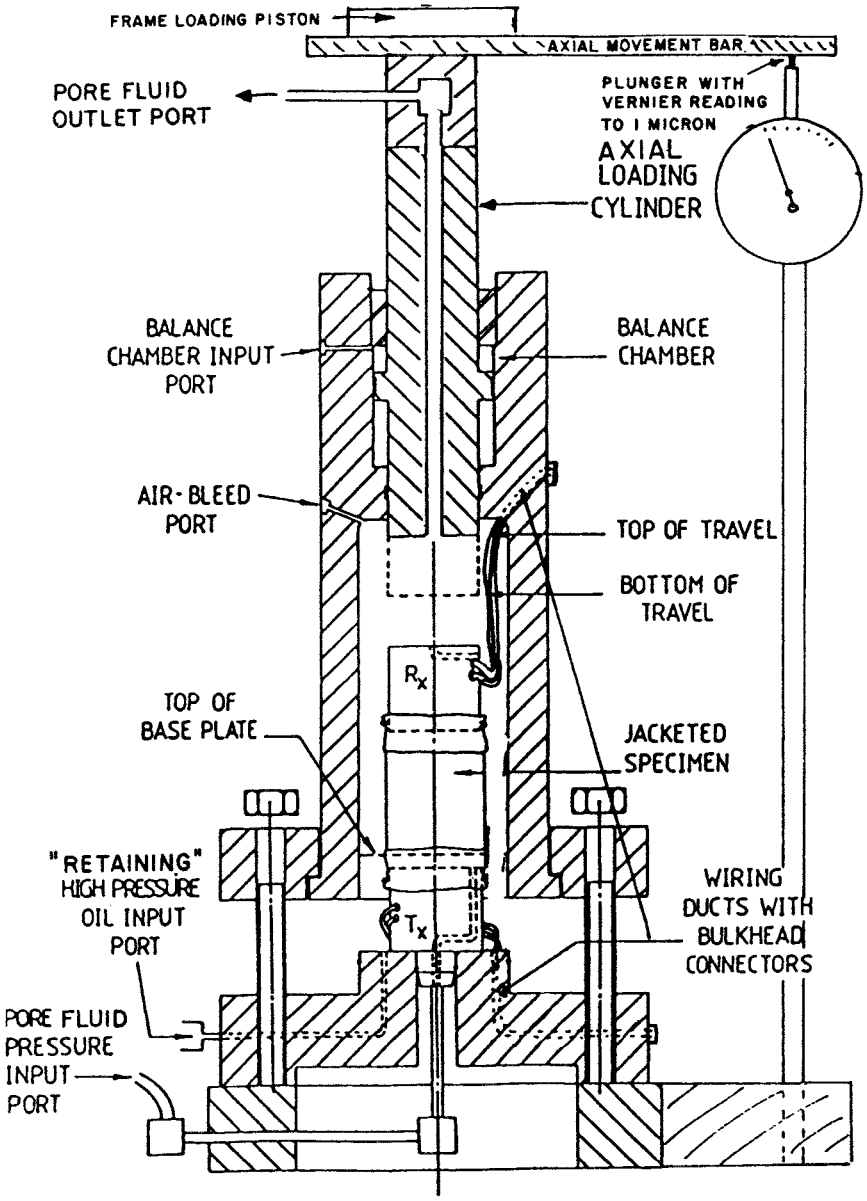

FIGURE 3 Cross-Section through the Hoek cell

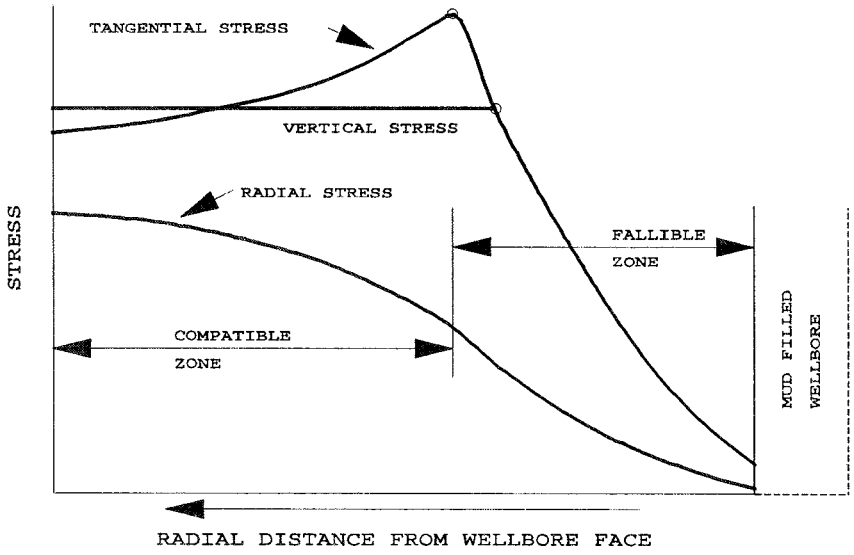

FIGURE 4A Distribution of effective stresses for unconsolidated sand.

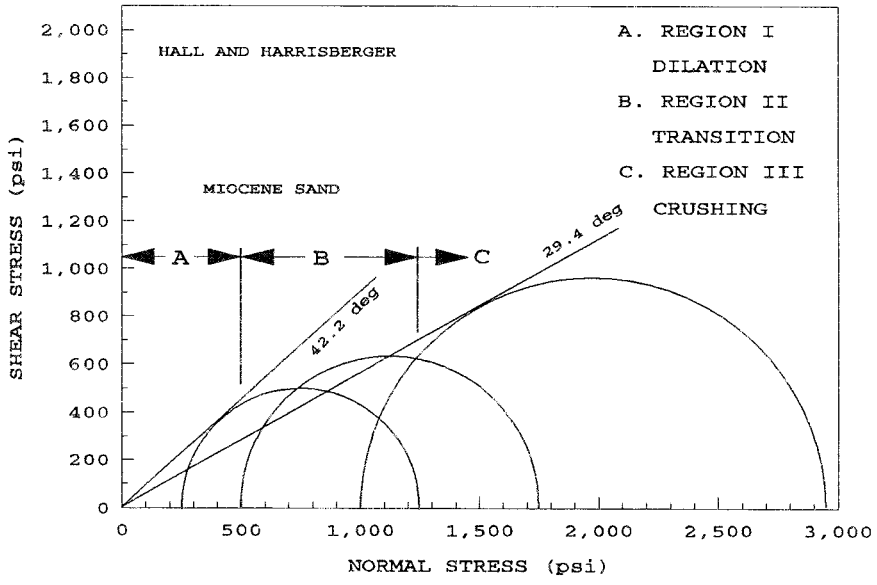

FIGURE 4B Near wellbore "non-elastic model" for effective stress and strain.

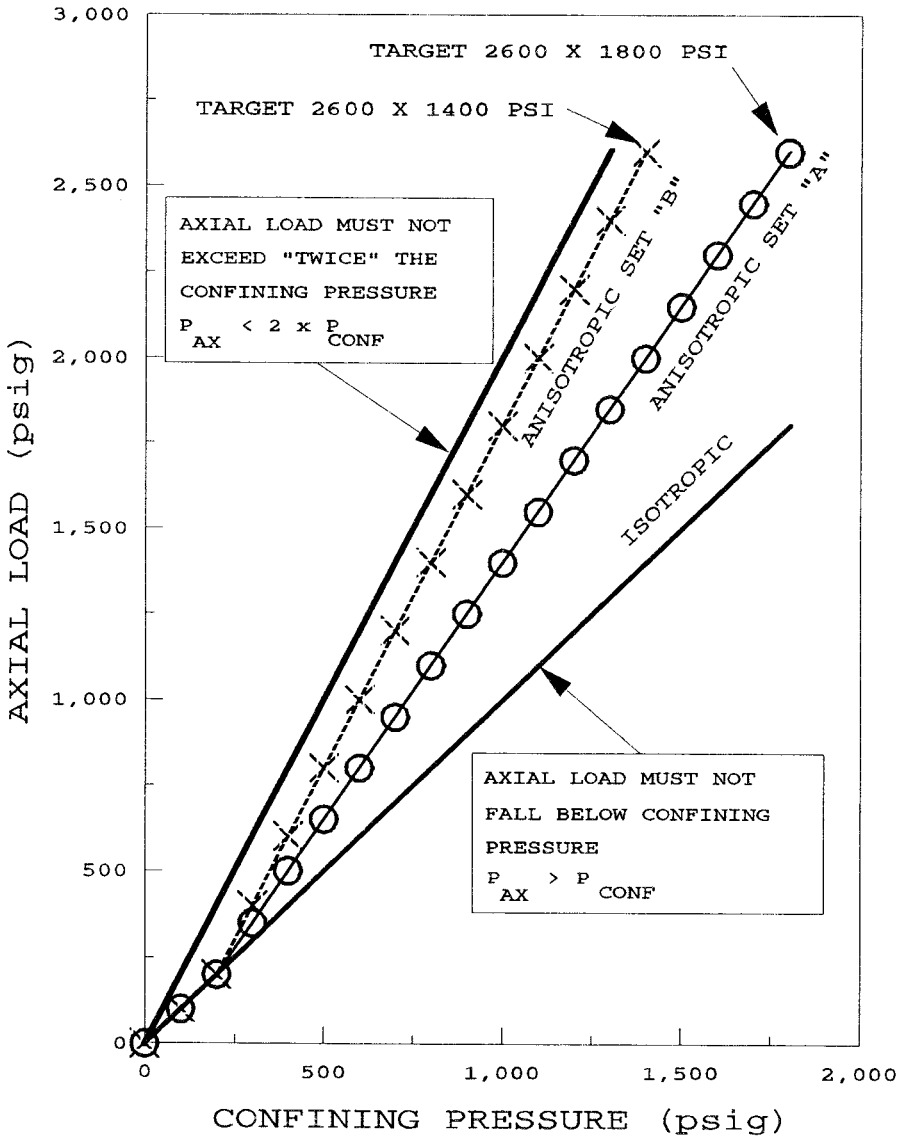

FIGURE 5 **Loading and unloading chart, as supplied to laboratories.**

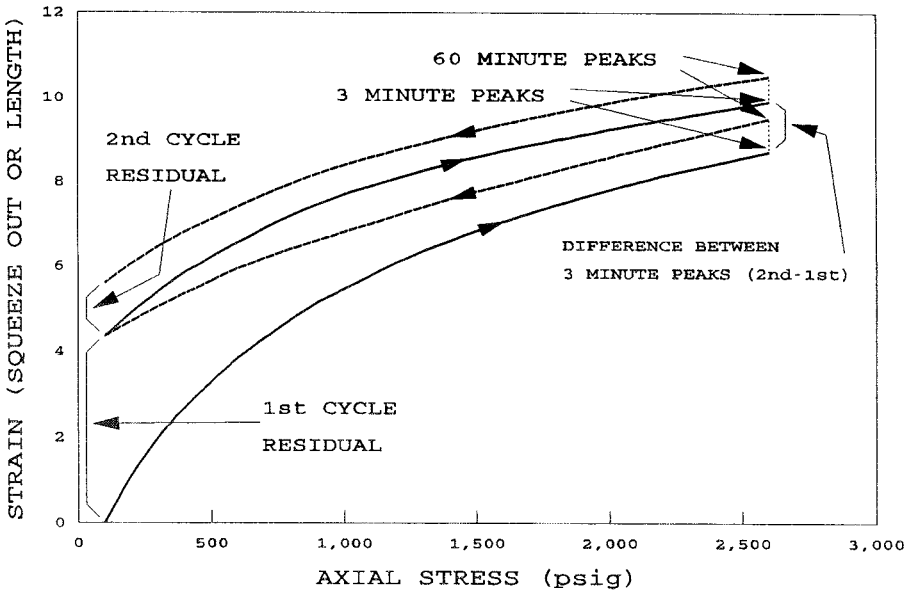

FIGURE 6 Typical stress-strain graph.

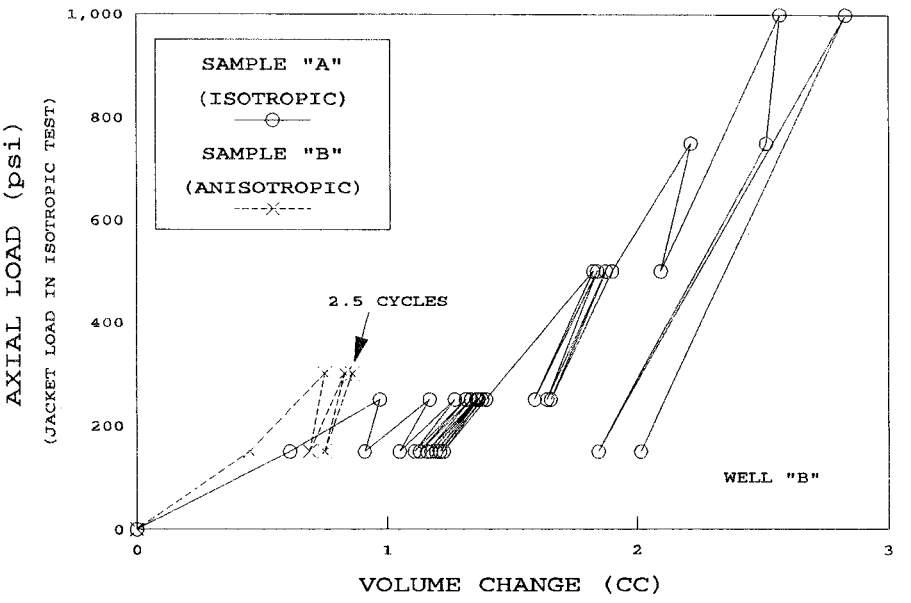

FIGURE 7 Trial stress and strain testing results - Well B.

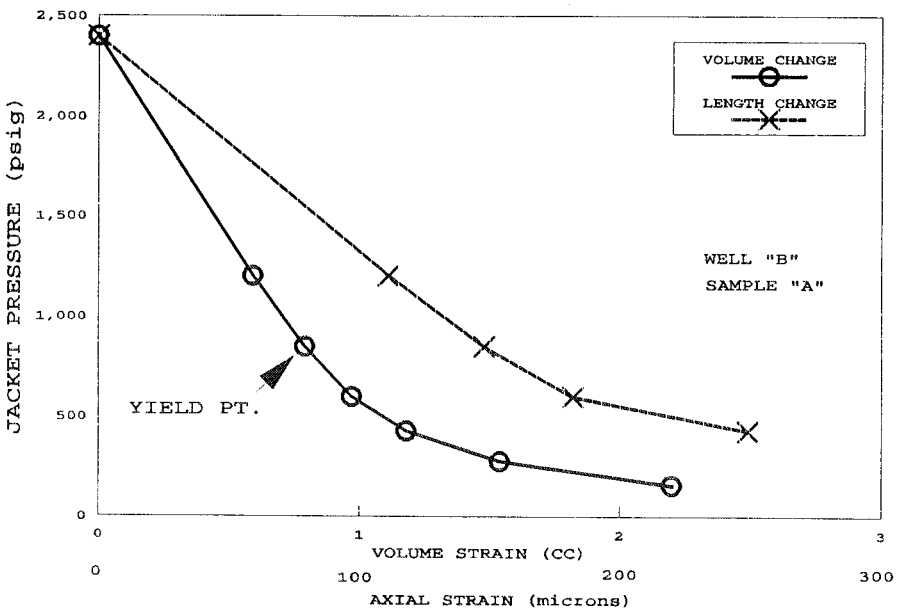

FIGURE 8 **Unloading by jacket pressure reduction, Sample "a" - Well B.**

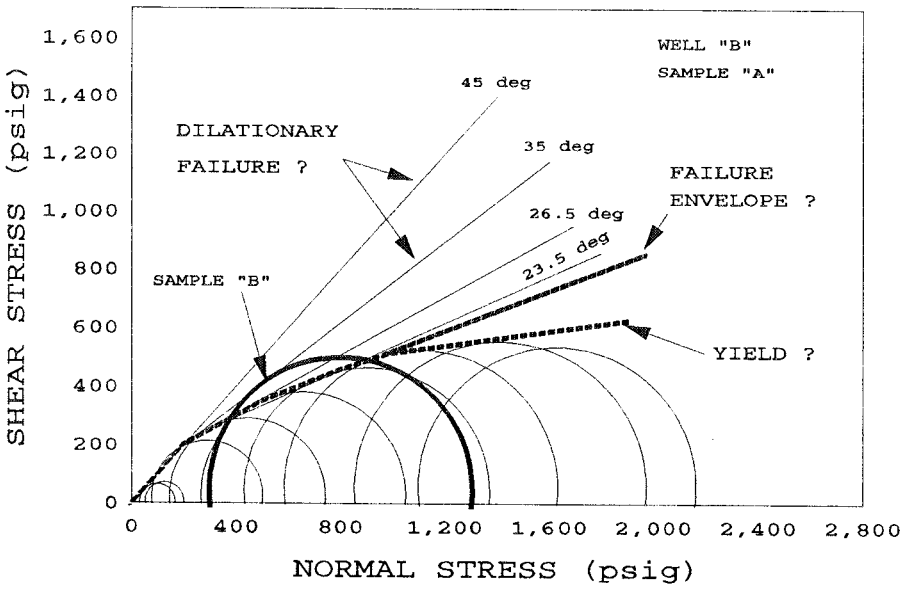

FIGURE 9 **Drained triaxial test results, Sample "a" - Well B.**

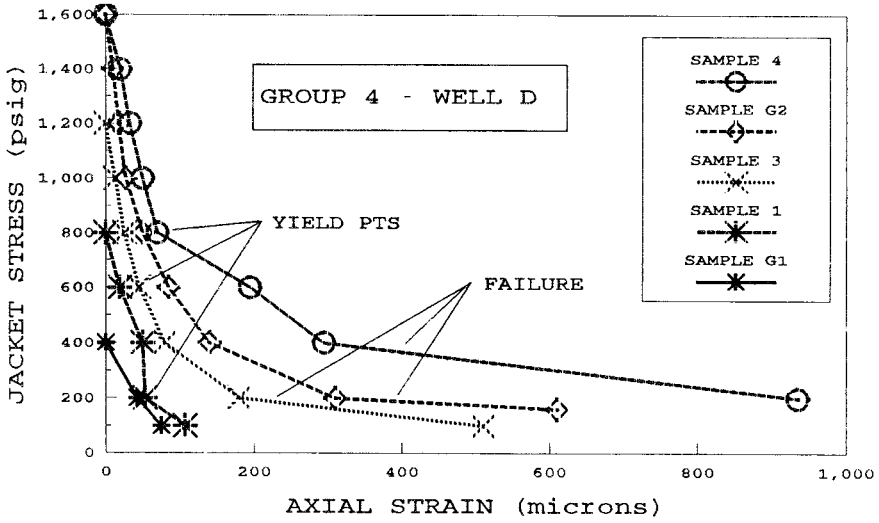

FIGURE 10 Typical stress/strain results, Sample Group 4 - Well D.

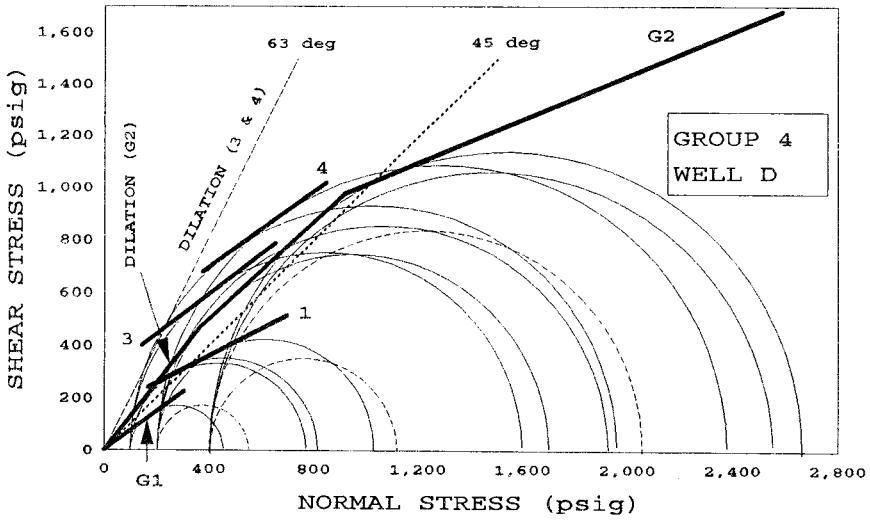

FIGURE 11 Typical Mohr's diagram, Sample Group 4 - Well D.